Fungal Genetics and Biology 52 (2013) 20–31

Contents lists available at SciVerse ScienceDirect

Fungal Genetics and Biology

journal homepage: www.elsevier.com/locate/yfgbi

Phylogenetic analyses of *RPB1* and *RPB2* support a middle Cretaceous origin for a clade comprising all agriculturally and medically important fusaria

Kerry O'Donnell [a,*], Alejandro P. Rooney [b], Robert H. Proctor [a], Daren W. Brown [a], Susan P. McCormick [a], Todd J. Ward [a], Rasmus J.N. Frandsen [c], Erik Lysøe [d], Stephen A. Rehner [e], Takayuki Aoki [f], Vincent A.R.G. Robert [g], Pedro W. Crous [g], Johannes Z. Groenewald [g], Seogchan Kang [h], David M. Geiser [h]

[a] *Bacterial Foodborne Pathogens and Mycology Research Unit, National Center for Agricultural Utilization Research, US Department of Agriculture, Agricultural Research Service, 1815 North University Street, Peoria, IL 61604, USA*
[b] *Crop Bioprotection Research Unit, National Center for Agricultural Utilization Research, US Department of Agriculture, Agricultural Research Service, 1815 North University Street, Peoria, IL 61604, USA*
[c] *Department of Systems Biology, Technical University of Denmark, 2800 Kgs. Lyngby, Denmark*
[d] *Department of Plant Health and Plant Protection, Bioforsk–Norwegian Institute of Agricultural and Environmental Research,1432 Ås, Norway*
[e] *Systematic Mycology and Microbiology Laboratory, United States Department of Agriculture, Agricultural Research Service, Beltsville, MD 20705, USA*
[f] *National Institute of Agrobiological Sciences, Genetic Resources Center, 2-1-2 Kannondai, Tsukuba, Ibaraki 305-8602, Japan*
[g] *CBS-KNAW Fungal Biodiversity Centre, Uppsalalaan 8, 3584 CT, Utrecht, Netherlands*
[h] *Department of Plant Pathology & Environmental Microbiology, The Pennsylvania State University, University Park, PA 16802, USA*

ARTICLE INFO

Article history:
Received 27 September 2012
Accepted 20 December 2012
Available online 26 January 2013

Keywords:
Evolution
Fumonisins
Gibberellins
Molecular dating
Mycotoxins
Trichothecenes

ABSTRACT

Fusarium (Hypocreales, Nectriaceae) is one of the most economically important and systematically challenging groups of mycotoxigenic phytopathogens and emergent human pathogens. We conducted maximum likelihood (ML), maximum parsimony (MP) and Bayesian (B) analyses on partial DNA-directed RNA polymerase II largest (*RPB1*) and second largest subunit (*RPB2*) nucleotide sequences of 93 fusaria to infer the first comprehensive and well-supported phylogenetic hypothesis of evolutionary relationships within the genus and 20 of its near relatives. Our analyses revealed that *Cylindrocarpon* formed a basal monophyletic sister to a 'terminal *Fusarium* clade' (TFC) comprising 20 strongly supported species complexes and nine monotypic lineages, which we provisionally recognize as *Fusarium* (hypothesis F1). The basal-most divergences within the TFC were only significantly supported by Bayesian posterior probabilities (B-PP 0.99–1). An internode of the remaining TFC, however, was strongly supported by MP and ML bootstrapping and B-PP (hypothesis F2). Analysis of seven *Fusarium* genome sequences and Southern analysis of fusaria elucidated the distribution of genes required for synthesis of 26 families of secondary metabolites within the phylogenetic framework. Diversification time estimates date the origin of the TFC to the middle Cretaceous 91.3 million years ago. We also dated the origin of several agriculturally important secondary metabolites as well as the lineage responsible for Fusarium head blight of cereals. Dating of several plant-associated species complexes suggests their evolution may have been driven by angiosperm diversification during the Miocene. Our results support two competing hypotheses for the circumscription of *Fusarium* and provide a framework for future comparative phylogenetic and genomic analyses of this agronomically and medically important genus.

Published by Elsevier Inc.

1. Introduction

Fusarium species rank among the most economically destructive plant pathogens and mycotoxigenic fungi, posing a threat to plant and animal health and food safety. Notable plant diseases include Fusarium head blight (FHB) or scab of cereals (O'Donnell et al., 2000; Cuomo et al., 2007), sudden death syndrome (SDS) of soybeans (Aoki et al., 2005), ear rot of maize (Desjardins et al., 2002), root rot of pea (Coleman et al., 2009), and vascular wilts of scores of economically important crops (O'Donnell et al., 1998b; Skovgaard et al., 2001; van der Does et al., 2008). Fusarium-induced losses to crop yield and quality, as well as contamination with mycotoxins, are responsible for multi-billion US dollar losses to world agriculture annually (Wu, 2007). In addition, fusaria are responsible for keratitis (Chang et al., 2006) and finger and toenail infections in immunocompetent humans, as well as life-threatening infections in humans with chronically low levels of white blood cells (Sutton and Brandt, 2011).

* Corresponding author. Fax: +1 309 681 6672.
E-mail address: kerry.odonnell@ars.usda.gov (K. O'Donnell).

1087-1845/$ - see front matter Published by Elsevier Inc.
http://dx.doi.org/10.1016/j.fgb.2012.12.004

Most phylogenetic studies conducted within the genus have focused on resolving evolutionary relationships at the species level within clades of agriculturally and medically important fusaria (GCPSR; Taylor et al., 2000; O'Donnell et al., 2010 and references therein). In the most comprehensive phylogenetic assessment of the genus to date, Gräfenhan et al. (2011) analyzed a two-locus data set from 43 fusaria and 50 hypocrealean near relatives. They discovered that 17 of the fusaria were nested within basal lineages comprising non-fusaria, strongly indicating that *Fusarium*, as traditionally defined (Gerlach and Nirenberg, 1982), is polyphyletic. Although the remaining 26 fusaria included in their study formed eight strongly supported lineages, designated the 'terminal *Fusarium* clade' (TFC), support for this lineage was poor and evolutionary relationships within it were unresolved. At least seven teleomorph genera are connected taxonomically to the TFC (Geiser et al., 2013); however, these sexual states are rarely encountered by applied biologists working on fusarial diseases and toxins. In revising teleomorph genera within the TFC, and assigning the name *Fusarium* for unitary use to replace only one of them, Gräfenhan et al. (2011) and Schroers et al. (2011) set up an inevitable splitting of the TFC into at least nine genera, despite the fact that almost all of the species in the TFC produce *Fusarium* anamorphs, which historically are the principal form by which these organisms are recognized and reported.

Given this background, we conducted the most comprehensive phylogenetic assessment of *Fusarium* to date using portions of the DNA-directed RNA polymerase II largest (*RPB1*) and second largest (*RPB2*) subunits, which are noted for their informativeness in analyses of diverse fungi (Schoch et al., 2009), including *Fusarium* (O'Donnell et al., 2010). Our goals were to (i) infer evolutionary relationships within the TFC to determine whether it is monophyletic, (ii) assess how well the traditional morphology-based subgeneric sectional classification corresponds to the molecular phylogeny, and (iii) construct the first time scale for the evolutionary origin and diversification of fusaria. Herein *Fusarium* is defined phylogenetically as a genealogically exclusive clade that is synonymous with the 'terminal *Fusarium* clade' (TFC sensu Gräfenhan et al., 2011). Thus, all of the species within the TFC are considered to be fusaria, irrespective of whether they produce a *Fusarium*-like anamorph. Given the economic importance of *Fusarium* and its toxins to world agriculture and food safety, the well-supported evolutionary framework developed in the present study should help guide future comparative phylogenetic and genomic studies on this genus.

2. Materials and methods

2.1. Taxon sampling and molecular phylogenetics

The 113 isolates included in this study (Supplementary Table S1) were chosen to represent the known morphological (Gerlach and Nirenberg, 1982) and phylogenetic diversity of *Fusarium* (O'Donnell et al., 2010; Gräfenhan et al., 2011). DNA extraction, PCR amplification and DNA sequencing followed published protocols (O'Donnell et al., 2010). Based on the results of model tests (Posada, 2008), the GTR + Γ + I default model of molecular evolution was selected for the ML-BS analyses, which were run with GARLI ver. 1.0 (Zwickl, 2006) on the CIPRES Science Gateway site (http://www.phylo.org/portal2/login). Clade support (Table 1) was assessed by: (i) nonparametric ML-BS using GARLI ver. 1.0 on CIPRES, (ii) maximum parsimony bootstrapping (MP-BS) in PAUP* ver. 4.0b10 (Swofford, 2003), employing 1000 pseudoreplicates of the data, 10 random taxon-addition sequences per replicate, TBR branch swapping, and MAXTREES set to automatically increase by 100, and (iii) Bayesian posterior probabilities using MrBayes ver. 3.1.2 (Huelsenbeck and Ronquist, 2001; Ronquist and Huelsenbeck, 2003) on the University of Oslo Bioportal (https://www.bioportal.uio.no/appinfo/show.php?app=mrbayes). Two Bayesian analyses of four chains were run for 5×10^7 generations, sampling trees every 100 generations. Inspection of t files generated from the analyses indicated chains had reached stationarity within the first quarter of each run so 12,500 trees from each run were discarded as the burn-in sample. To obtain posterior probabilities (PPs), the 37,500 trees from each run were combined into a single tree file that was imported into PAUP to obtain 85% and 95% majority-rule consensuses.

DNA sequence data generated in this study have been deposited in GenBank (accession numbers JX171444–JX171669) and the concatenated two-locus alignment was deposited in TreeBASE (accession number S12813, Tree number Tr56612). To promote DNA sequence-based identification through web-based tools, all of the data reported in this study have been incorporated into *Fusarium*-ID (Geiser et al., 2004; Park et al., 2010) and *Fusarium MLST* (O'Donnell et al., 2010).

2.2. Secondary metabolites

The presence of secondary metabolite biosynthetic genes was assessed using three methods: (i) BLAST analysis of published genome sequences of *Fusarium graminearum* (Cuomo et al., 2007), *Fusarium pseudograminearum* (Gardiner et al., 2012), *Fusarium oxysporum*, *Fusarium verticillioides* (Ma et al., 2010) and '*Fusarium solani*' (Coleman et al., 2009) and unpublished genome sequences of *Fusarium avenaceum* and *Fusarium langsethiae* (Frandsen and Lysøe, unpubl. results) (Table 2); (ii) SOUTHERN blot analysis of selected polyketide synthase (PKS) genes of multiple isolates representing seven species complexes (Supplementary Table S3); and (iii) reports in the literature for which rigorous methods were used to determine species identities, e.g., comparisons of DNA sequences of unknown strains to those of previously validated strains. Because the correct species name for the isolate of '*F. solani*' ('*Nectria*' *haematococca* mating population VI) used for genome sequencing is unknown, it is listed with single quotation marks.

Table 1
Tree statistics and summary sequence for individual and combined partitions (see Figs. 1 and 2).

Locus	# Characters	# MPTs[a]	MPT length	CI[b]	RI[c]	UIC[d]	PIC[e]	PIC/bp[f]	# Nodes supported [g]		
									MP-BS	ML-BS	PP
RPB1	1606	8	8747	0.19	0.68	50	827	0.51	85	87	91
RPB2	1777	6	8913	0.18	0.67	44	802	0.45	78	80	89
Combined	3383	4	17,738	0.18	0.67	94	1629	0.48	94	99	104

[a] MPTs, most-parsimonious or shortest trees.
[b] CI, consistency index.
[c] RI, retention index.
[d] UIC, parsimony-uniformative, autapomorphic, or uniquely derived character.
[e] PIC, parsimony-informative, synapomorphic or shared derived character.
[f] PIC/bp, parsimony-informative characters/base pair.
[g] Number of nodes supported by maximum parsimony bootstrapping (MP-BS), maximum likelihood bootstrapping (ML-BS) and Bayesian posterior probability (PP).

Table 2
Distribution of secondary metabolite biosynthetic genes in genome sequences of fusaria representing the *sambucinum* (*F. graminearum*, *F. pseudograminearum*, *F. langsethiae*), *tricinctum* (*F. avenaceum*), *fujikuroi* (*F. verticillioides*), *oxysporum* (*F. oxysporum*) and *solani* ('*F. solani*') species complexes.

Metabolite	Gene designation[a]	Accession[b]	Genome[c]						
			Fgram NRRL 31084	*Fpseu* CS3096	*Flang* NRRL 54940	*Faven* NRRL 54939	*Fvert* NRRL 20956	*Foxys* NRRL 34936	*Fsola* NRRL 45880
Polyketides									
Aurofusarin	*AUR1*	FGSG_02324	+	+	+/–[d]	+	–	–	–
Bikaverin	*BIK1*	AJ278141	–	–	–	–	+	+/–	–
Depudecin	*DEP5*	FVEG_01736	–	–	+	–	+*	+*/–	–
Equisetin	*eqiS*	AY700570	–	–	–	–	–	–	–
Fumonisins	*FUM1*	FVEG_00316	–	–	–	–	+	+/–	–
Fusarielin	*FSL1*	FGSG_10464	+	+	–	–	–	–	–
Fusaric acid	*FUB1*	FVEG_12523	–	–	–	–	+	+	–
Fusarins	*FUS1*	FGSG_07798	+	+	+*	+	+	–	+*
Perithecial pigment-red	*pksN*	33672	–	–	–	–	–	–	+
Perithecial pigment-violet	*PGL1*	FGSG_09182	+	+	+*	+	+	+	+
Zearalenone	*ZEA1*	FGSG_15980	+	+	–	–	–	–	–
Zearalenone	*ZEA2*	FGSG_17745	+	+	–	–	–	–	–
Unknown	*PKS7*	FGSG_08795	+*	+*	+*	+*	+*	+*	+*
Unknown	*PKS8*	FGSG_03340	+*	+*	+*	+*	+*	+*	+*
Nonribosomal peptides									
Beauvericin/Enniatin	*ESYN*[d]	Z18755	–	–	+*	+	–	+	–
Ferricrocin	*SidC*	FGSG_05372	+*	+*	+*	+*	+*	+*	+*
Fusarinine	*SidD*	FGSG_03747	+*	+*	+*	+*	+*	+*	+*
Malonichrome	*NRPS1*	FGSG_11026	+*	+*	+*	+*	+*	+*	+*
Unknown	*NRPS3*	FGSG_10523	+*	+*	+*	+*	+*	+*	+*
Unknown	*NRPS4*	FGSG_02315	+*	+*	+*	+*	+*	+*	+*
Unknown	*NRPS10*	FGSG_06507	+*	+*	+*	+*	+*	+*	+*
Unknown	*NRPS11*	FGSG_03245	+*	+*	+*	+*	+*	+*	+*
Unknown	*NRPS12*	FGSG_17574	+*	+*	+*	+*	+*	+*	+*
Terpenes									
Culmorin	*CLM1*	FGSG_10397	+	+	–	+*	–	–	–
Gibberellins	*cps*/*ks*[e]	Y15013	–	–	+*	+*	–	+*/–	–
Trichothecenes	*TRI5*	FGSG_03537	+	+	+	–	–	–	–
Other									
Butenolide	FGSG_08079	FGSG_08079	+	+	–	+	–	–	–

[a] *PKS* and *NRPS* gene designations have been described (Hansen et al., 2012). Information on gene designations and links between metabolites and genes have been described previously: *AUR1*/*PKS12*, *PGL1* and *ZEA1* (Gaffoor et al., 2005); *BIK1* (Wiemann et al., 2009); *DEP5* (Wight et al., 2009); *eqiS* (Sims et al., 2005); *FUM1* (Proctor et al., 2006); *FUB1* and *FUS1* (Brown et al., 2012); *pksN* (Graziani et al., 2004); *ESYN* (Herrmann et al., 1996; Xu et al., 2012); *SidC* (Tobiasen et al., 2007); *SidD* (Varga et al., 2005); *CLM1* (McCormick et al., 2010); *cps*/*ks* (Tudzynski, 2002); *TRI5* (Alexander et al., 2009); FGSG_08079 (Harris et al., 2007).

[b] Sequence accessions used for BLAST. FGSG, FOXG and FVEG indicate accessions for *F. graminearum*, *F. oxysporum* and *F. verticillioides*, respectively, in the Broad Institute Fusarium Comparative Database. 33672 (*pksN*) is from the *Nectria –haematococca* ('*F. solani*') database at the Joint Genome Institute. Accessions AJ278141 (*BIK1*), AY700570 (*EqiS*), Y15013 (*cps*/*ksd*), and Z18755 (*ESYN*) are from the National Center for Biotechnology Information database.

[c] Species name abbreviations: *Fgram* – *F. graminearum*; *Fpseu* – *F. pseudograminearum*; *Flang* – *F. langsethiae*; *Faven* – *F. avenaceum*; *Fvert* – *F. verticillioides*; *Foxys* – *F. oxysporum*; and *Fsola* – '*F. solani*'. + indicates gene was detected in genome sequence database; – indicates gene was not detected; +/– indicates gene was detected in sequences of some isolates but not in others. The exception is *AUR1*; it was not detected in the genome sequence of *F. langsethiae*; but, other isolates can produce aurofusarin and therefore must have *AUR1* (Thrane et al., 2004). * indicates metabolite production has not been confirmed.

[d] Although FVEG_09993 exhibits 66% sequence identity to *Fusarium equiseti ESYN* and *Beauveria BeaS* (Herrmann et al., 1996; Xu et al., 2012), it is likely a pseudogene because it lacks a condensation domain-encoding region. The *F. verticillioides* genome sequence also lacks a ketoisovalerate reductase gene (*kivR*). The condensation domain and *kivR* are essential for beauvericin and enniatin biosynthesis (Xu et al., 2012).

[e] Homologs of the gibberellin biosynthetic gene genes *cps*/*ks* and *ggs* were detected in the *F. langsethiae* genome, but homologs of other gibberellin genes were not detected. Homologous of all gibberellin genes, except for *P450-3*, were detected in *F. avenaceum* (Frandsen and Lysøe, unpubl. results).

2.3. Divergence-time estimates

BEAST ver. 1.7.1 (Drummond and Rambaut, 2007) was used to generate divergence time estimates from the partial *RPB1* and *RPB2* nucleotide sequences based on a Bayesian approach. Sequences of *Candida albicans*, *Saccharomyces cerevisiae*, *Magnaporthe grisea*, *Schizosaccharomyces pombe* and *Aspergillus flavus* were used as calibration points as per Sung et al. (2008) and Gueidan et al. (2011). These taxa were chosen as representatives of the clades dated in the aforementioned studies to provide *a priori* divergence dates for BEAST analyses and from which a rate estimate was obtained and subsequent dates were generated for nodes in the phylogeny. Analyses were run under (i) an uncorrelated lognormal relaxed molecular clock with the calibrated Yule model (Heled and Drummond, 2012) as the tree prior (Fig. 2); and (ii) an uncorrelated lognormal relaxed molecular clock with the birth–death model (Gernhard, 2008) as the tree prior (Supplementary Fig. S2). All other priors and operators were allowed to auto-optimize. Estimates of the posterior distribution of clade age and rates were obtained using a Markov Chain Monte Carlo (MCMC) run for 500 million generations, sampling every 500,000 generations. BEAST output was visualized with TRACER ver. 1.5 (Rambaut and Drummond, 2007) and the MCMC was determined to have reached convergence when all effective sample sizes were greater than 300. The results were summarized as maximum clade credibility (MCC) trees (Drummond and Rambaut, 2007) using Tree Annotator ver. 1.7.1. Statistical uncertainty of divergence time estimates in the MCC trees was assessed by the 95% highest probability density (HPD) intervals (i.e., Bayesian equivalent of a confidence interval).

3. Results

3.1. Phylogenetic diversity of Fusarium

MP bootstrapping of the individual *RPB1* and *RPB2* data sets resolved 85 and 78 nodes, respectively, with ⩾70% MP-BS. In addition to 71 of the same nodes in both trees being supported by MP-BS, no strongly supported clades were in positive conflict. MP analysis of the combined data set conducted with PAUP* (Swofford, 2003) yielded four equally most-parsimonious trees (MPTs) 17,738 steps in length (Fig. 1; Table 1); the best ML tree ($-\mathrm{Ln}L$ score = 79111.37) obtained using GARLI (Zwickl, 2006) was highly concordant with the MPTs. The four MPTs were identical except for minor rearrangements of *Fusarium torulosum* and *Fusarium floccciferum* within the *tricinctum* species complex. As expected, MP and ML bootstrap analyses of the combined partitions identified more internodes with ⩾70% support (94 and 99) than did analyses of the individual *RPB1* (85 and 87) and *RPB2* (78 and 80) data sets. With the exception of four internodes along the backbone of the phylogeny and five within the interior of the tree that received <70% MP and ML bootstrap values (indicated by thick red internodes in Fig. 1), the MPT represents a highly resolved estimate of *Fusarium* phylogeny.

The two basal-most branches within the outgroup-rooted phylogeny comprised six non-*Fusarium* clades (Fig. 1, highlighted in gray). The earliest diverging lineage comprised five strongly supported (99% ML-BS, 76% MP-BS, B-PP 1) clades, four of which contain taxa that were recently segregated from *Fusarium* (Gräfenhan et al., 2011). The next clade to diverge within the phylogeny was represented by species with *Cylindrocarpon* anamorphs, which was resolved with moderate to strong support (84% ML-BS, B-PP 1) as sister to the TFC. We recognize this clade as one of two competing hypotheses of the phylogenetic limits of the genus *Fusarium* (i.e., F1 in Figs. 1 and 2; Geiser et al., in press). Twenty species complexes and nine monotypic lineages were resolved within the TFC (i.e., *Fusarium* sensu hypothesis F1). Although five of the internodes near the base of the *Fusarium* phylogeny were not supported by MP and ML bootstrapping (Figs. 1, 2A and B), four of these received B-PP values of 0.99–1 (indicated by red asterisks in Fig. 2C). Thus, our hypothesis of evolutionary diversification of the six most basal lineages within *Fusarium* is based almost exclusively on the Bayesian analysis. The latter analysis resolved the *ventricosum* species complex as the basal most divergence within *Fusarium* (B-PP 0.99), followed by the *dimerum*, *albidum*, and *staphyleae* species complexes (Fig. 2C). Red arrowheads designated F1 or F2 identify internodes supporting the inclusion of the *ventricosum* and *albidum* species complexes, respectively (Figs. 1 and 2A), which represent alternate hypotheses of *Fusarium*. In contrast to the limited support (B-PP 1, ML and MP bootstrapping <70%) for hypothesis F1, internode F2 was strongly supported by ML and MP bootstrapping (100% and 87%, respectively), and by a B-PP of 1. In addition, 18 of the 20 informally named species complexes within the TFC were strongly supported (⩾88% ML-BS, ⩾79% MP-BS, B-PP 1 (Fig. 1)). The *fujikuroi* and *oxysporum* species complexes were subtended by short internodes that received only moderate measures of support. However, internodes connecting each of these clades to their sister taxa (i.e., *fujikuroi* to *Fusarium* sp. NRRL 52700 and *oxysporum* to *Fusarium foetens*) were strongly supported by all three measures of clade support. In addition to the undescribed *Fusarium* sp. NRRL 52700 and *F. foetens*, seven other phylogenetically divergent species appeared to be novel monotypic lineages (Fig. 1).

To directly compare our results based on the *RPB1* + *RPB2* data set with the *RPB2* + ATP citrate lyase (*acl1*) data set used in Gräfenhan et al. (2011), we reanalyzed the latter data set via ML, MP and Bayesian methods. This reanalysis did not resolve the sister group of *Fusarium* nor relationships among the eight basal-most species complexes (Fig. 2D). However, lowering the stringency of the majority-rule consensus in the Bayesian analysis from 95% to 85% identified four nodes with B-PP values between 0.88 and 0.94 (Fig. 2D).

The *RPB1* + *RPB2* molecular phylogeny has provided the first robust genus-wide framework for evaluating whether the traditional morphology-based sectional classification (Gerlach and Nirenberg, 1982) accurately reflects evolutionary relationships within *Fusarium*. Most of the clades identified here cut across *Fusarium* sectional boundaries, as illustrated by color-coding taxa previously classified in one of the 17 morphologically defined sections (Fig. 1). A majority of the 20 fusaria not classified in sections (i.e., not color-coded in Fig. 1) were recently described using molecular phylogenetics. *Fusarium rusci* and *Fusarium neocosmosporiellum*, which are nested within the TFC, were previously classified, respectively, in *Pycnofusarium* (Hawksworth and Punithalingam, 1973) and *Neocosmospora* (Smith, 1899).

3.2. Phylogenetic distribution of secondary metabolites

The presence of secondary metabolite biosynthetic (SMB) genes responsible for synthesis of 26 families of metabolites was evaluated by surveying genome sequences of seven *Fusarium* species (Table 2) and by Southern blot analysis of selected PKS genes in a wider range of 41 species (Table S3). The resulting information was used to assess the likely origin and phylogenetic distribution of the corresponding secondary metabolites in the context of the two-locus phylogeny of *Fusarium* (Fig. 1). Our analyses used PKS, nonribosomal peptide synthase (NRPS) and terpene cyclase genes as markers for SMB gene clusters, because these genes encode enzymes that catalyze the first committed step in SMB pathways. The genome sequence and Southern blot analyses revealed marked variation in the distribution of SMB genes, and therefore variation in genetic potential to produce the corresponding secondary metabolites. Several SMB genes have narrow phylogenetic

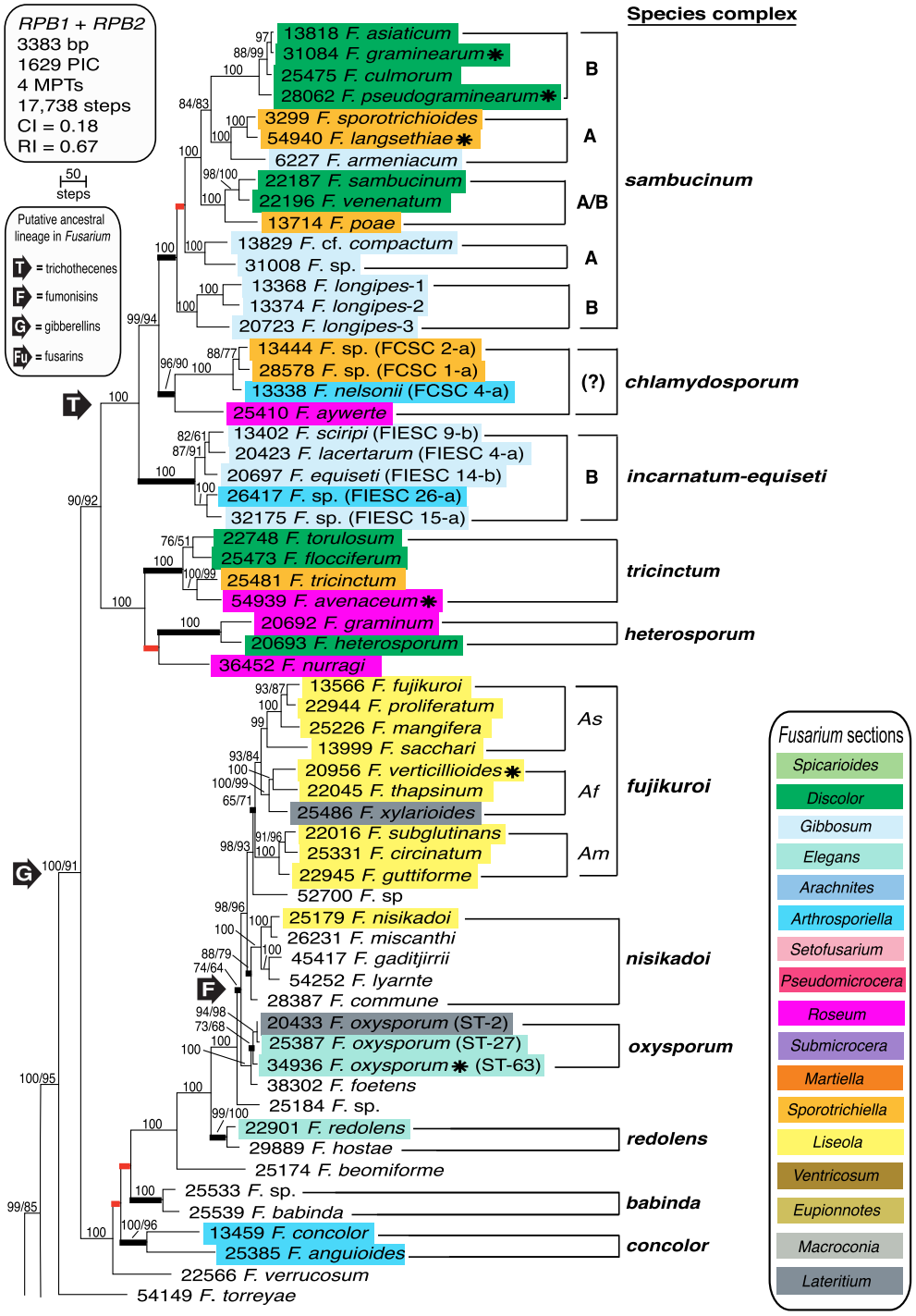

Fig. 1. One of four most-parsimonious trees inferred from parsimony analysis of combined *RPB1* + *RPB2* data set, rooted on sequences of *Sphaerostilbella aureonitens* and *Hypocrea* sp. (Hypocreaceae). Each species is identified by a unique ARS Culture Collection (NRRL) accession number. Thickened black branches identify six basal non-*Fusarium* lineages (highlighted in light gray) and 20 strongly supported, informally named species complexes within *Fusarium* (=terminal *Fusarium* clade [TFC] sensu Gräfenhan et al., 2011). Red arrowheads labeled F1 and F2 represent alternate hypotheses of *Fusarium* that require further testing. F1 (=TFC) was only significantly supported by a B-PP of 0.99, whereas internode F2 was supported by three separate measures of clade support (i.e., 100% ML-BS, 87% MP-BS, B-PP 1). Numbers above internodes represent maximum likelihood (ML) and maximum parsimony (MP) bootstrap support (ML-BS/MP-BS); only a single value is indicated when they were identical. Thickened red branches identify nine internodes that were not supported by ML and MP bootstrapping (<70% support). Taxa are color-coded according to prior classification in morphologically defined sections (Gerlach and Nirenberg, 1982). Bold black asterisks identify seven species whose whole genome sequences were surveyed for secondary metabolite gene clusters (Table 2). Labeled black arrows identify the earliest known presence of four secondary metabolite gene clusters in *Fusarium* (T = trichothecenes, F = fumonisins, Fu = fusarins, G = gibberellin); note these do not represent ancestral state reconstructions because the data is very preliminary and incomplete and because some of the clusters may have been transmitted horizontally. A and/or B type trichothecene production is mapped onto *sambucinum* subclades and *incarnatum-equiseti* species complex. Though sharing a MRCA with the latter two species complexes, (–) indicates trichothecene toxin production has not been demonstrated by members of *chlamydosporum* species complex. Three biogeographically structured subclades within *fujikuroi* species complex are identified as follows: *As* = Asian, *Af* = African, *Am* = American. Arabic numbers and lowercase Roman letters are used to identify multilocus species and haplotypes, respectively, within *chlamydosporum* and *incarnatum-equiseti* species complexes and clade 3 of *solani* species complex. In addition, two-locus (IGS rDNA + *EF-1α*) sequence types (STs) are included for members of *oxysporum* species complex (O'Donnell et al., 2009). *Fusarium longipes* 1–3 and *F. ventricosum* 1–3 indicate that each morphospecies is represented by three phylogenetically distinct species.

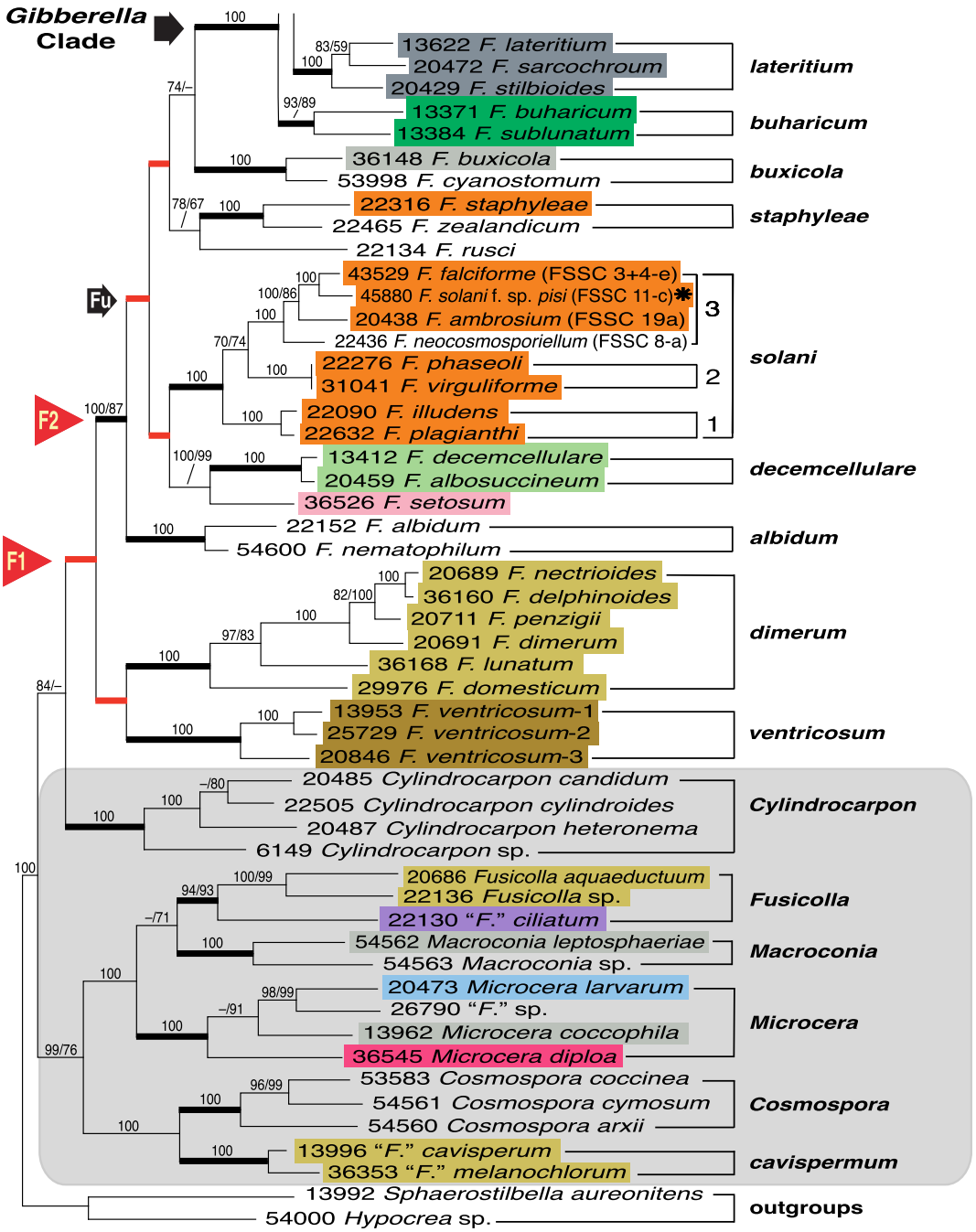

Fig. 1. (*continued*)

distributions. Fumonisin and bikaverin biosynthetic genes, for example, were detected only within the *fujikuroi* and *oxysporum* species complexes (Table 2, Supplemental Table S3, Fig. 1). Some SMB genes exhibited an even more restricted distribution. Specifically, the fusarielin and zearalenone PKS genes were detected only in *F. graminearum* and *F. pseudograminearum* and the red perithecial pigment biosynthetic gene, *pksN*, only in the *solani* species complex (Table 2); however, presence of these genes was assessed only in the seven genome sequences and not by Southern analysis.

The survey of genome sequences also revealed that some clusters, or at least parts of clusters, are distributed more widely than previously thought. This is evident from the presence of gibberellin biosynthetic genes in *F. langsethiae*, *F. avenaceum*, and *F. oxysporum*, which are, respectively, members of the *sambucinum*, *tricinctum*, and *oxysporum* species complexes (Table 2). Also, phylogenetically diverse fusaria have the genetic potential to produce fusaric acid as is evident by the presence of the fusaric acid PKS gene in members of the *fujikuroi*, *nisikadoi*, *oxysporum* and *redolens* species complexes (Table 2, Supplementary Table S3). The PKS gene required for production of fusarin mycotoxins was detected in an even wider range of fusaria (i.e., *sambucinum*, *incarnatum-equiseti*, *tricinctum*, *fujikuroi*, *nisikadoi*, *redolens* and *solani* species complexes) (Table 2, Supplementary Table S3). According to both Southern blot and genome sequence surveys, the PKS gene (*PGL1*), which is required for synthesis of fusarubins, as well as *PKS7* and *PKS8* were present in all species examined across distantly related species complexes (i.e., *sambucinum*, *incarnatum-equiseti*, *tricinctum*, *fujikuroi*, *nisikadoi*, *oxysporum*, *redolens* and *solani*). Similarly, eight

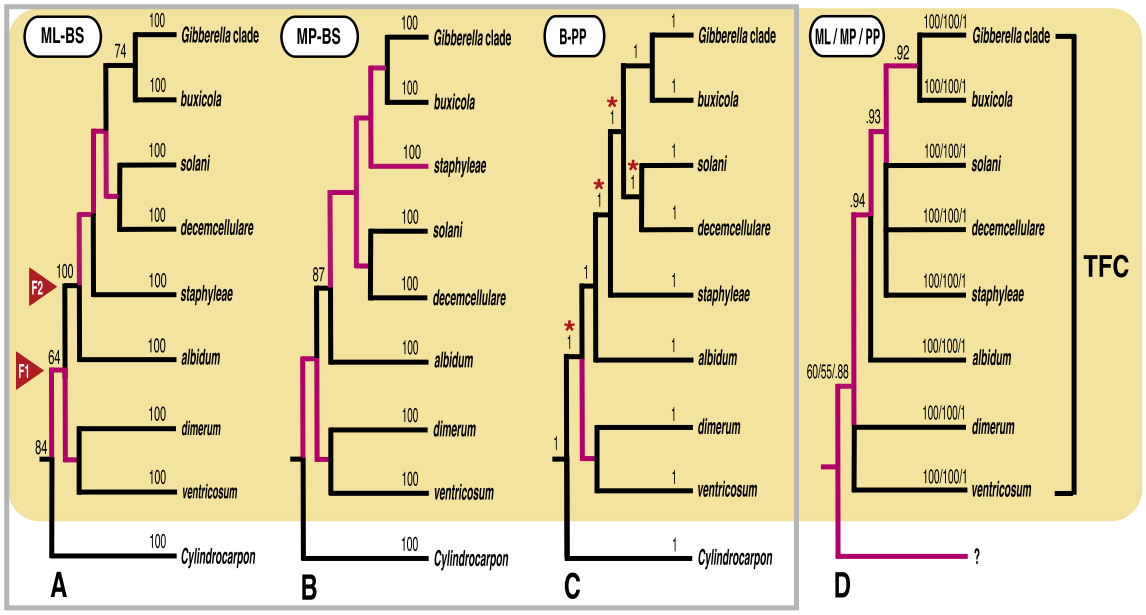

Fig. 2. (A–C). Stylized trees summarizing (A) ML-BS, (B) MP-BS, and (C) Bayesian-PP for terminal *Fusarium* clade (TFC) obtained from analyses of combined *RPB1* + *RPB2* data set. Red branches indicate they were unresolved. Red asterisks identify four nodes that were not supported by bootstrapping but were significantly supported by Bayesian posterior probabilities (B-PP) of 0.99–1. In all analyses, *Cylindrocarpon* was supported as sister to TFC. (A) Alternate hypotheses of *Fusarium* are indicated by red arrowheads labeled F1 and F2. (D) Reanalysis of Gräfenhan et al. (2011) two-locus data set revealed that the data resolved neither the sister of nor any relationship within TFC. Because no branch was supported by a B-PP ⩾ 0.95, an 85% majority-rule consensus was constructed.

of the nine nonribosomal peptide synthase (NRPS) genes queried were detected in all seven *Fusarium* genomes surveyed. The one exception was the NRPS gene responsible for beauvericin and enniatin synthesis; this gene was absent in *F. graminearum* and '*F. solani*' and it was a pseudogene in *F. verticillioides*.

3.3. Divergence-time estimates of Fusarium

Our analyses suggest that the terminal *Fusarium* clade (TFC) diverged from its sister group *Cylindrocarpon* in the middle Cretaceous 91.3 Mya [95% HPD interval: 44.7, 149.3] (Fig. 3, node 1) and the eight basal-most lineages within the TFC, including the *Gibberella* clade, evolved by the late Eocene 48.9 Mya [95% HPD interval: 22.7, 79.0]. If we assume the biosynthetic gene clusters were transmitted vertically after fusaria acquired them, then the phylogeny suggests that the ability to produce fusarin mycotoxins was present in *Fusarium* by the late Cretaceous 66.6 Mya [95% HPD interval: 31.8, 108.2] in the most recent common ancestor (MRCA) of the 17 most recently derived species complexes (Fig. 3, node 4), gibberellins since the late Eocene 38.0 Mya [95% HPD interval: 18.4, 61.8] in the MRCA of the 11 most recently derived species complexes (Fig. 3, node 8), trichothecenes by the late Oligocene 26.5 Mya [95% HPD interval: 12.8, 44.7] in the MRCA of the *incarnatum-equiseti*, *chlamydosporum* and *sambucinum* species complexes (Fig. 3, node 11), and fumonisins in the MRCA of the *fujikuroi* and *oxysporum* species complexes by the late Miocene 11.0 Mya [95% HPD interval: 5.1, 18.3] (Fig. 3, node 12). The two-locus phylogeny strongly supported a sister-group relationship between the *chlamydosporum* and *sambucinum* species complexes, suggesting that the former clade's potential to produce trichothecenes has either been lost, despite maintenance of an intact *TRI5* gene (O'Donnell, unpubl. results), or gone undetected. Also, the chronogram supports a late Miocene evolutionary origin of the predominately grass-associated *nisikadoi* species complex 9.7 Mya [95% HPD interval: 4.3, 15.9] (Fig. 1, node 13). In addition, radiation of the B Clade (i.e., *F. graminearum*, *F. asiaticum*, *F. culmorum* and *F. pseudograminearum* in Fig. 1), which produce B trichothecenes, was dated to the middle Pliocene 3.4 Mya [95% HPD interval: 1.2, 6.5] (Fig. 3, node 17), suggesting that the trichothecene gene cluster has been under strong balancing selection, as proposed by Ward et al. (2002), for at least 3.4 My. The chronogram also suggests the homothallic FHB pathogens within the *F. graminearum* species complex (i.e., *F. graminearum* and *F. asiaticum*) diverged from their heterothallic ancestors in the Pleistocene 1.7 Mya [95% HPD interval: 0.5, 3.4] and subsequently radiated recently, 0.8 Mya [95% HPD interval: 0.2, 1.8] (Fig. 3, nodes 19 and 20].

4. Discussion

4.1. Phylogenetic diversity of Fusarium

Results of the present study provide the first strong Bayesian support for a monophyletic 'terminal *Fusarium* clade' (TFC) that we present as one of two hypotheses (i.e., F1 in Figs. 1–3) of the phylogenetic limits of this genus. Because the internode corresponding to F1 was only significantly supported in Bayesian analysis (B-PP 0.99), and the next diverging lineage was supported by all three measures of clade support, we designated the latter internode as hypothesis F2 (see Figs. 1–3). Even though Gräfenhan et al. (2011) previously described and named the TFC, no internode approximating F1 and F2 was strongly supported in their two-locus phylogeny. By way of contrast, ML and MP bootstrapping significantly supported three internodes within the TFC in our two-locus phylogeny (Fig. 2A and B) and our Bayesian phylogeny was fully resolved (i.e., B-PP 0.99–1 in Fig. 2C).

Because significantly more internodes were strongly supported in the bootstrap (⩾9–19) and Bayesian analyses (⩾13–15) of the combined data, the two-locus phylogeny represents our best estimate of evolutionary relationships within *Fusarium* and its near relatives. As noted in previous studies (reviewed in Lumbsch et al. (2005)), we found that four internodes were only significantly supported by Bayesian posterior probabilities and this is particularly evident among the basal most lineages of the TFC. However, given the observed correlation between bootstrap values and

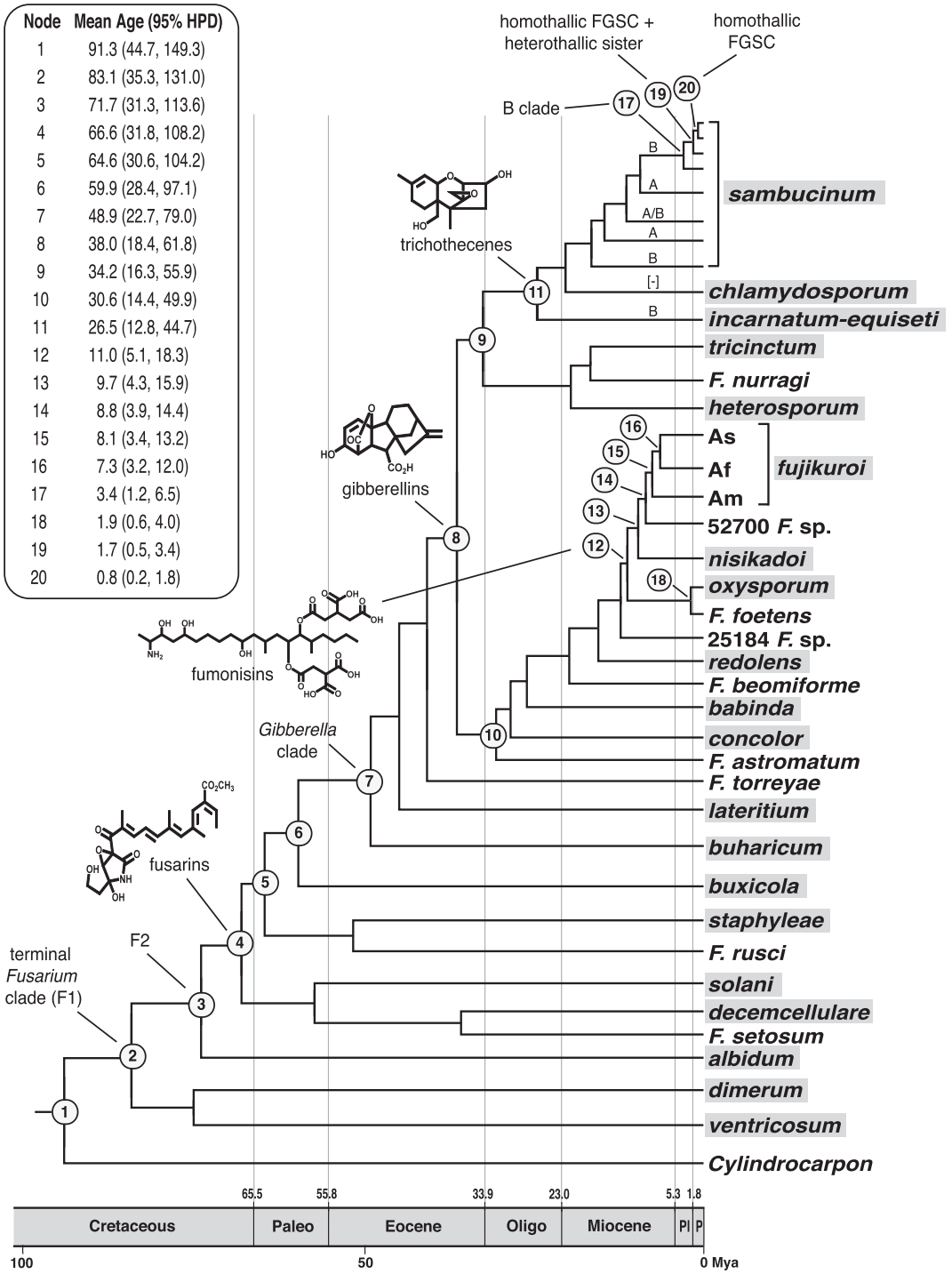

Fig. 3. Maximum clade credibility (MCC) tree showing divergence age estimates for major lineages of *Fusarium* generated using calibrated Yule model (see Supplementary Fig. S2 for data generated using birth–death model). Numbered circles identify 20 nodes for which divergence times are reported; 10 nodes are labeled to identify evolutionary origin of six lineages, and four secondary metabolites. Names in gray boxes represent species complexes. Published divergence times for five calibration taxa were used to estimate divergence times (see Section 2). Calibration taxa and all non-*Fusarium* lineages except for *Cylindrocarpon* spp. were pruned from the chronogram to focus on *Fusarium*; however, calibration taxa are included in MCC trees obtained using the birth–death and calibrated Yule models, respectively, as Supplementary Figs. S3 and S4. The terminal *Fusarium* clade (F1, node 2) and F2 (see node 3) represent alternate hypotheses of *Fusarium* (see bottom half of Fig. 1). Geological time scale is in millions of years before present (Mya, Walker et al., 2009). FGSC = *Fusarium graminearum* species complex (Sarver et al., 2011), HPD = highest probability density interval, Paleo = Paleocene, Pl = Pliocene, P = Pleistocene.

posterior probabilities, we predict that the former will converge on the latter as additional phylogenetically informative genes in *Fusarium* are sampled.

The present study significantly extends our knowledge of *Fusarium* phylogenetic diversity from 8 to 10 medically and agriculturally important clades (O'Donnell et al., 2010; Gräfenhan et al., 2011; Watanabe et al., 2011) to 20 informally named species complexes and nine monotypic lineages. While we do not advocate nor see the need to formally recognize the clades as subgenera, the names of species complexes were nevertheless selected based on

nomenclatural priority or their use in prior studies (O'Donnell et al., 2010). Consistent with the findings of Kristensen et al. (2005) and Watanabe et al. (2011), the robust phylogenetic framework developed in the present study suggests that the traditional morphology-based sectional classification scheme adopted in previous taxonomic treatments of *Fusarium* (Wollenweber and Reinking, 1935; Booth, 1971; Gerlach and Nirenberg, 1982; Nelson et al., 1983) is artificial. As noted by Gräfenhan et al. (2011), the iconic multiseptate, fusiform macroconidium is not synapomorphic for *Fusarium* as circumscribed here; however, classic *Fusarium* macroconidia are produced by a large majority of species within the TFC.

4.2. Phylogenetic circumscription of Fusarium

Our discovery of strong support for a 'terminal *Fusarium* clade' (TFC) and corresponding phylogenetic structure within it has important implications for *Fusarium* taxonomy as Dual Nomenclature ends (Hawksworth et al., 2011). Gräfenhan et al. (2011) proposed that unitary use of *Fusarium* be confined to the *Gibberella* Clade. If this was done, the remaining species in the TFC, including the agriculturally and medically important *solani* species complex, must be segregated into at least nine genera and lose their nomenclatural connection to *Fusarium*. Instead, we offer two phylogenetic-based classification hypotheses that are more closely aligned with user opinion, demand and established use: one hypothesis for a unitary *Fusarium* that includes all species within the TFC (i.e., F1 in Figs. 1–3) and another that limits *Fusarium* such that the *albidum* species complex is the most basal member of the genus (i.e., F2 in Figs. 1–3). The logic for using the *Fusarium* anamorph to typify this clade is guided by the following: (i) the nodes labeled as F1 and F2 are both supported as monophyletic, (ii) it promotes taxonomic stability by avoiding unnecessary name changes, (iii) a large majority of fungi circumscribed by F1 and F2 produce fusiform macroconidia, the most familiar trait by which agricultural and medical mycologists recognize *Fusarium*, and (iv) *Fusarium* Link as sanctioned by Fries (Fries, 1821) is a much older name with nomenclatural priority over all teleomorph names. Given the uncertainty as to whether *Fusarium* corresponds to hypothesis F1 or F2, we recommend that hypothesis F1 (i.e., TFC sensu Gräfenhan et al., 2011) be used until more phylogenetically informative data resolve this question.

4.3. Phylogenetic distribution of secondary metabolites

The presence and absence of SMB genes in fusaria in the context of the phylogenetic framework and divergence times has provided novel insights into *Fusarium* secondary metabolism, particularly with respect to when *Fusarium* acquired the ability to produce some metabolites (Fig. 1). The results also indicate marked variation in the distribution of SMB genes among species and species complexes. In some cases (e.g., gibberellin biosynthetic genes), the distribution of SMB genes, and therefore potential for metabolite production, is more widespread than previously noted (Bömke and Tudzynski, 2009). Furthermore, although some SMB genes appear to occur uniformly across *Fusarium*, discontinuous distribution of SMB genes is common regardless of whether the genes occur in only one or a few (e.g., fumonisin and bikaverin genes) or widely across many (e.g., fusarin genes) species complexes. The cause of this discontinuity (homoplasy) likely varies for different SMB clusters. Deletion of part or all of the gibberellin and fumonisin biosynthetic gene clusters in several fusaria indicates that gene deletion can contribute to SMB homoplasy in some cases (Bömke and Tudzynski, 2009; Van Hove et al., 2011). However, transfer of chromosomes between species or interspecific hybridization could also contribute to homoplasy of SMB clusters and secondary metabolite production (Coleman et al., 2009; Ma et al., 2010; Studt et al., 2012a).

The present study is the first to robustly place the *chlamydosporum* species complex within the lineage of trichothecene-producing fusaria (Fig. 1). Although sequence analysis of *TRI5* amplicons from multiple species within the *chlamydosporum* clade suggests this trichothecene biosynthetic gene is likely functional, none of the five isolates examined produced trichothecenes under standard laboratory conditions (McCormick and Proctor, unpubl.). Further analyses are required to determine whether members of this species complex have lost the ability to produce trichothecenes or produce them under more restricted conditions than members of the *sambucinum* and *incarnatum-equiseti* complexes.

In addition to their discontinuous distribution, phylogenetic relationships of homologous SMB genes are not always correlated with species phylogenies (Ward et al., 2002; Proctor et al., 2009). Given this, the value of SMB genes as a taxonomic tool for *Fusarium* is limited. Nevertheless, secondary metabolism can influence the understanding of relationships between fusaria. Nowhere is this more evident than with perithecial pigmentation, which varies among fusaria and is used as a taxonomic character (Gräfenhan et al., 2011; Schroers et al., 2011). For example, fusaria with a *Gibberella* teleomorph produce black/dark violet perithecia while some (e.g., '*F. solani* f. sp. *pisi*') with a *Nectria*-like teleomorph produce red perithecia. In fusaria with a *Gibberella* teleomorph, the six-gene *PGL* cluster confers the blackish pigmentation of perithecia (Gaffoor et al., 2005; Proctor et al., 2007; Studt et al., 2012b). The red pigmentation of '*F. solani* f. sp. *pisi*' perithecia is conferred by a cluster consisting of at least one PKS (*pksN*) and one monooxygenase gene (*ppcA*) (Graziani et al., 2004; Vasnier et al., 2005). Although '*F. solani* f. sp. *pisi*' also has a *PGL* cluster (Proctor et al., 2007; Brown et al., 2012), it most likely does not contribute to perithecial pigmentation in this species, because deletion of *pksN* or *ppcA* results in colorless perithecia (Graziani et al., 2004; Vasnier et al., 2005). Naturally occurring, colorless perithecia in *Fusarium decemcellulare*, *Fusarium albidum*, and *Fusarium verrucosum* were used to place all three species in the teleomorph genus *Albonectria* (Rossman et al., 1999). However, the phylogenies reported here and in Gräfenhan et al. (2011) indicate that these species are phylogenetically diverse and, therefore, that colorless perithecia likely evolved independently in multiple lineages of *Fusarium*. Based on available data, we posit that colorless perithecia in these three fusaria resulted from loss or altered expression of the biosynthetic gene clusters that confer red and blackish perithecial pigmentation. In contrast, both and/or additional pigment biosynthetic clusters may be active in *Fusarium buxicola* and *Fusarium staphyleae*, which produce perithecia that are both red and blackish (Gräfenhan et al., 2011; Schroers et al., 2011).

4.4. Divergence-time estimates of Fusarium

Dated fungal phylogenies, including the one hypothesized here for *Fusarium*, are subject to several sources of error (Taylor and Berbee, 2006; Berbee and Taylor, 2010), and this is reflected in the broad confidence intervals on many nodes in the chronogram (Fig. 3). The two main sources of error include fossil calibrations and rate heterogeneity among lineages (Taylor and Berbee, 2006). To account for any potential discrepancies in lineage-specific rate differences, we used an uncorrelated lognormal relaxed clock model (Drummond and Rambaut, 2007). With respect to the former, one source of error in our divergence-time estimates is lack of a relatively recent (e.g., less than 25 Mya) calibration point. Given the rarity of fungal fossils, the only other potential source of fossil calibration points for an analysis of divergence times would be fungi preserved in fossilized amber (e.g., Sung et al., 2008). Because such data were not available, we were

restricted to using older calibration dates (i.e., >100 Mya). Another potential source of error is use of single species as calibration taxa. However, age estimates used in our calibration were taken from published studies that utilized multiple species for the same higher-level calibration taxa that we chose to represent with individual species. In that sense, our calibration points, in spite of being represented by only single species, are more reliable than had we used them (as single species/sequence representatives) to generate *de novo* age estimates for calibration points.

Taking into account all of these caveats, our analyses suggest that *Fusarium* originated in the middle Cretaceous (Fig. 3, node 1; and Supplementary Fig. S2) and the four basal-most lineages diversified before but survived the Cretaceous–Tertiary mass extinction event. Given the close association of diverse fusaria with plants, and the plant-based ancestral nutritional state inferred for hypocrealean fungi (Sung et al., 2008), we conjecture that the spectacular angiosperm radiation in the Cretaceous, and subsequent burst of evolution during the mid-to-late Miocene, played a central role in the evolutionary diversification of *Fusarium*. Two lines of evidence suggest that fusaria may have evolved initially on woody hosts: early Cretaceous flora primarily consisted of woody anthophytes and shrubby angiosperms (Soltis et al., 2008; Smith et al., 2010), and most of the early diverging lineages of *Fusarium* contain lignicolous species that may be endophytic, parasitic or saprophytic.

The available data suggest that the four secondary metabolite gene clusters mapped on the phylogeny either evolved by vertical inheritance from a hypocrealean ancestor or were transferred horizontally in *Fusarium* during different epochs (see Fig. 3), with fusarins dated to the late Cretaceous, gibberellins to the early Eocene, trichothecenes to the late Oligocene, and fumonisins to the middle Miocene (see Fig. 3). Furthermore, the chronogram suggests that the B clade of trichothecene toxin-producing fusaria, in which the trichothecene gene cluster has been shown to be subject to strong balancing selection (Ward et al., 2002), radiated in the middle Pliocene 3.4 Mya [95% HPD interval: 1.2, 6.5] (Fig. 3, node 17). The little or no variation detected within the ITS rDNA region among members of the *fujikuroi* species complex (Fig. 3, node 15; mean age 8.1 Mya; O'Donnell et al., 1998a), and more recently evolved lineages such as the *F. graminearum* species complex (FGSC in Fig. 3, node 20; mean age 0.8 Mya), confirm that this locus is evolving too slowly to resolve the 50 and 16 species, respectively, within these agronomically important lineages. As such, our results suggest that the ITS region may not be useful in resolving fusaria that diverged relatively recently (e.g., less than 10 Mya).

Our time-calibrated phylogeny strongly contradicts the proposed vicariance of Gondwanaland to explain the origin of the *fujikuroi* species complex's three biogeographically structured subclades (O'Donnell et al., 1998a). To the contrary, the *Fusarium* chronogram supports a post-Gondwanan origin of the *fujikuroi* species complex in the late Miocene 8.8 Mya [95% HPD interval: 3.9, 14.4] (Fig. 3, node 14) rather than during the Cretaceous approximately 100 Mya earlier. To explain the pseudo-congruent shared area relationships (Donoghue and Moore, 2003), the most-parsimonious scenario appears to involve long distance dispersal from South America to Africa, followed by a transoceanic dispersal from Africa to Asia in the late Miocene. In addition, our results indicate that five of the most agronomically important and species-rich clades (i.e., *fujikuroi*, *incarnatum-equiseti*, *sambucinum*, *solani*, *tricinctum* species complexes), which include most of the mycotoxigenic and phytopathogenic fusaria, began to diversify during the middle-to-late Miocene. Thus, we posit that diversification of these fusaria may have been linked to the concomitant explosive radiation of grasses and eudicots that use C_4 photosynthesis to fix carbon (Edwards et al., 2010; Christin et al., 2011). As noted for diverse plants and animals (Sanmartín et al., 2001; Donoghue and Smith, 2004), our dated phylogeny also suggests that late Miocene cooling and desertification may have fragmented ancestral species ranges, thereby contributing to the significant species radiations within *Fusarium* during this epoch. The origin and diversification of the predominately grass-associated *nisikadoi* species complex was dated to the Miocene 9.7 Mya (Fig. 3, node 13), after grasslands had become dominant worldwide (Kellogg, 2001). While relatively little is known about the diversity within this species complex, it includes epi- and endophytes of Andropogoneae, Bambuseae and Pooideae, including species that are transmitted vertically in seeds. Although the *oxysporum* species complex collectively comprises the largest group of phytopathogenic fusaria (O'Donnell et al., 2009), they represent a surprisingly recent radiation dated to the late Pliocene 1.9 Mya [95% HPD interval: 0.6, 4.0] (Fig. 3, node 18). Equally surprising is the relatively recent evolutionary origin and radiation of the homothallic FHB pathogens within the *F. graminearum* species complex, which appear to have split from their heterothallic ancestors in the early Pleistocene 1.7 Mya [95% HPD interval: 0.5, 3.4] (Sarver et al., 2011) (Fig. 3, nodes 19 and 20). Given the Pleistocene evolutionary origin inferred for these cereal pathogens, the phylogenetic results suggest that their divergence predated the domestication of grasses, as previously noted for smut pathogens of sorghum, maize and sugarcane (Munkacsi et al., 2007).

Acknowledgments

We are pleased to acknowledge the excellent technical support of Stacy Sink for generating DNA sequence data presented in this study, Nathane Orwig for running sequences in the NCAUR DNA Core Facility, Marcie Moore for conducting Southern blot analyses and Kimberly MacDonald for preparing cultures for toxin analysis. Thanks are due Tom Gräfenhan for providing his two-locus data set for our reanalysis. The mention of firm names or trade products does not imply that they are endorsed or recommended by the US Department of Agriculture over other firms or similar products not mentioned. The USDA is an equal opportunity provider and employer.

Appendix A. Supplementary data

Supplementary data associated with this article can be found, in the online version, at http://dx.doi.org/10.1016/j.fgb.2012.12.004.

References

Alexander, N.J., Proctor, R.H., McCormick, S.P., 2009. Genes, gene clusters, and biosynthesis of trichothecenes and fumonisins in *Fusarium*. Toxin Rev. 28, 198–215.

Aoki, T., O'Donnell, K., Scandiani, M., 2005. Sudden death syndrome of soybean in South America is caused by four species of *Fusarium*: *Fusarium brasiliense* sp. nov., *F. cuneirostrum* sp. nov., *F. tucumaniae* and *F. virguliforme*. Mycoscience 46, 162–183.

Berbee, M.L., Taylor, J.W., 2010. Dating the molecular clock in fungi – how close are we? Fungal Biol. 24, 1–16.

Bömke, C., Tudzynski, B., 2009. Diversity, regulation, and evolution of the gibberellins biosynthetic pathway in fungi compared to plants and bacteria. Phytochemistry 70, 1876–1893.

Booth, C., 1971. The Genus *Fusarium*. Commonwealth Mycological Institute, Kew, England.

Brown, D.W., Butchko, R.A.E., Busman, M., Proctor, R.H., 2012. Identification of gene clusters associated with fusaric acid, fusarin, and perithecial pigment production in *Fusarium verticillioides*. Fungal Genet. Biol. 49, 521–532.

Chang, D.C., Grant, G.B., O'Donnell, K., Wannemuehler, K.A., Noble-Wang, J., et al., 2006. A multistate outbreak of *Fusarium* keratitis associated with use of a contact lens solution. JAMA 296, 953–963.

Christin, P.-A., Osborne, C.P., Sage, R.F., Arakaki, M., Edwards, E.J., 2011. C_4 eudicots are not younger than C_4 monocots. J. Exp. Bot. 62, 3171–3181.

Coleman, J.J., Rounsley, S.D., Rodriguez-Carres, M., Kuo, A., Wasmann, C.C., et al., 2009. The genome of *Nectria haematococca*: contribution of supernumerary chromosomes to gene expansion. PLoS Genet. 5, e1000618.

Cuomo, C.A., Guldener, U., Xu, J.-R., Trail, F., Turgeon, B.G., et al., 2007. The genome sequence of *Fusarium graminearum* reveals localized diversity and pathogen specialization. Science 317, 1400–1402.

Desjardins, A.E., Munkvold, G.P., Plattner, R.D., Proctor, R.H., 2002. *FUM1* – a gene required for fumonisin biosynthesis but not for maize ear rot and ear infection by *Gibberella moniliformis* in field tests. Mol. Plant–Microbe Interact. 15, 1157–1164.

Donoghue, M.J., Moore, B.R., 2003. Toward an integrative historical biogeography. Integr. Comp. Biol. 43, 261–270.

Donoghue, M.J., Smith, S.A., 2004. Patterns in the assembly of temperate forests around the northern Hemisphere. Philos. Trans. Roy. Soc. B. 359, 1633–1644.

Drummond, A.J., Rambaut, A., 2007. BEAST: Bayesian evolutionary analysis by sampling trees. BioMed. Evol. Biol. 7, 214. http://dx.doi.org/10.1186/1471-2148-7-214.

Edwards, E.J., Osborne, C.P., Strömberg, A.E., Smith, S.A., C4 Grasses Consortium, 2010. The origins of C4 grasslands: integrating evolutionary and ecosystem science. Science 328, 578–591.

Fries, E.M., 1821. Syst. Mycol. 1, xli (Introductio).

Gaffoor, I., Brown, D.W., Plattner, R.D., Proctor, R.H., Qi, W., et al., 2005. Functional analysis of the polyketide synthase genes in the filamentous fungus *Gibberella zeae* (anamorph *Fusarium graminearum*). Eukaryot. Cell 4, 1926–1933.

Gardiner, D.M., McDonald, M.C., Covarelli, L., Solomon, P.S., Rusu, A.G., et al., 2012. Comparative pathogenomics reveals horizontally acquired novel virulence genes in fungi infection cereal hosts. PLoS Pathog. 8 (9), e1002952, http://dx.doi.org/10.1094/PHYTO-07-12-0150-LE.

Geiser, D.M., Aoki, T., Bacon, C.W., Baker, S.E., Bhattacharyya, M.K., et al., 2013. LETTER TO THE EDITOR: One fungus, one name: Defining the genus *Fusarium* in a scientifically robust way that preserves longstanding use. Phytopathology.

Geiser, D.M., del Mar Jiménez-Gasco, M., Kang, S., Makalowska, I., Veeraraghavan, N., et al., 2004. FUSARIUM-ID v. 1.0: a DNA sequence database for identifying *Fusarium*. Eur. J. Plant Pathol. 110, 473–479.

Gernhard, T., 2008. The conditioned reconstructed process. J. Theor. Biol. 253, 769–778.

Gerlach, W., Nirenberg, H., 1982. The genus *Fusarium* – a pictorial atlas. Mitt. Biol. Bundesanst. Land-Forstwirtsch. Berlin-Dahlem 209, 1–406.

Gräfenhan, T., Schroers, H.-J., Nirenberg, H.I., Seifert, K.A., 2011. An overview of the taxonomy, phylogeny, and typification of nectriaceous fungi in *Cosmospora*, *Acremonium*, *Fusarium*, *Stilbella*, and *Volutella*. Stud. Mycol. 68, 79–113.

Graziani, S., Vasnier, C., Daboussi, M.-J., 2004. Novel polyketide synthase from *Nectria haematococca*. Appl. Environ. Microbiol. 70, 2984–2988.

Gueidan, C., Ruibal, C., de Hoog, G.S., Schneider, H., 2011. Rock-inhabiting fungi originated during periods of dry climate in the late Devonian and middle Triassic. Fungal Biol. 115, 987–996.

Hansen, F.T., Sørensen, J.L., Giese, H., Sondergaard, T.E., Frandsen, R.J.N., 2012. Quick guide to polyketide synthase and nonribosomal synthetase genes in *Fusarium*. Int. J. Food Microbiol. 155, 128–136.

Harris, L.J., Alexander, N.J., Saparno, A., Blackwell, B., McCormick, S.P., et al., 2007. A novel gene cluster in *Fusarium graminearum* contains a gene that contributes to butenolide synthesis. Fungal Genet. Biol. 44, 293–306.

Hawksworth, D.L., Crous, P.W., Redhead, S.A., Reynolds, D.R., Samson, R.A., et al., 2011. The Amsterdam declaration on fungal nomenclature. IMA Fungus 2, 105–112.

Hawksworth, D.L., Punithalingam, E., 1973. New and interesting microfungi from Slapton, south Devonshire, Deuteromycotina. Trans. Brit. Mycol. Soc. 61, 57–69.

Heled, J., Drummond, A.J., 2012. Calibrated tree priors for relaxed phylogenetics and divergence time estimation. Syst. Biol. 61, 138–149.

Herrmann, M., Zocher, R., Haese, A., 1996. Effect of disruption of the enniatin synthase gene on the virulence of *Fusarium avenaceum*. Mol. Plant–Microbe Interact. 9, 226–232.

Huelsenbeck, J.P., Ronquist, F., 2001. MRBAYES: Bayesian inference of phylogeny. Bioinformatics 17, 754–755.

Kellogg, E.A., 2001. Evolutionary history of the grasses. Plant Physiol. 125, 1198–1205.

Kristensen, R., Torp, M., Kosiak, B., Holst-Jensen, A., 2005. Phylogeny and toxigenic potential is correlated in *Fusarium* species as revealed by partial translation elongation factor 1 alpha gene sequences. Mycol. Res. 109, 173–186.

Lumbsch, H.T., Schmitt, I., Lindemuth, R., Miller, A., Mangold, A., et al., 2005. Performance of four ribosomal DNA regions to infer higher-level phylogenetic relationships of inoperculate euascomycetes (Leotiomyceta). Mol. Phylogenet. Evol. 34, 512–524.

Ma, L.-J., van der Does, H.C., Borkovich, K.A., Coleman, J.J., Daboussi, M.-J., et al., 2010. Comparative genomics reveals mobile pathogenicity chromosomes in *Fusarium*. Nature 464, 367–373.

McCormick, S.P., Alexander, N.J., Harris, L.J., 2010. *CLM1* of *Fusarium graminearum* encodes a longiborneol synthase required for culmorin production. Appl. Environ. Microbiol. 76, 136–141.

Munkacsi, A.B., Stoxen, S., May, G., 2007. Domestication of maize, sorghum, and sugarcane did not drive the divergence of their smut pathogens. Evolution 61, 388–403.

Nelson, P.E., Toussoun, T.A., Marasas, W.F.O., 1983. *Fusarium* Species: An Illustrated Manual for Identification. Pennsylvania State University Press, University Park, PA.

O'Donnell, K., Cigelnik, E., Nirenberg, H., 1998a. Molecular systematics and phylogeography of the *Gibberella fujikuroi* species complex. Mycologia 90, 465–493.

O'Donnell, K., Gueidan, C., Sink, S., Johnston, P.R., Crous, P.W., et al., 2009. A two-locus DNA sequence database for typing plant and human pathogens within the *Fusarium oxysporum* species complex. Fungal Genet. Biol. 46, 936–948.

O'Donnell, K., Kistler, H.C., Cigelnik, E., Ploetz, R.C., 1998b. Multiple evolutionary origins of the fungus causing Panama disease of banana: concordant evidence from nuclear and mitochondrial gene genealogies. Proc. Natl. Acad. Sci. USA 95, 2044–2049.

O'Donnell, K., Kistler, H.C., Tacke, B.K., Casper, H.H., 2000. Gene genealogies reveal global phylogeographic structure and reproductive isolation among lineages of *Fusarium graminearum*, the fungus causing wheat scab. Proc. Nat. Acad. Sci. USA 95, 7905–7910.

O'Donnell, K., Sutton, D.A., Rinaldi, M.G., Sarver, B.A.J., Balajee, S.A., et al., 2010. Internet-accessible DNA sequence database for identifying fusaria from human and animal infections. J. Clin. Microbiol. 48, 3708–3718.

Park, B., Park, J., Cheong, K.-C., Choi, J., Jung, K., et al., 2010. Cyber infrastructure for *Fusarium*: three integrated platforms supporting strain identification, phylogenetics, comparative genomics, and knowledge sharing. Nucl. Acids Res. 39, D640–D646.

Posada, D., 2008. JModelTest: phylogenetic model averaging. Mol. Biol. Evol. 25, 1253–1256.

Proctor, R.H., Butchko, R.A.E., Brown, D.W., Moretti, A., 2007. Functional characterization, sequence comparisons and distribution of a polyketide synthase gene required for perithecial pigmentation in some *Fusarium* species. Food Addit. Contam. 24, 1076–1087.

Proctor, R.H., McCormick, S.P., Alexander, N.J., Desjardins, A.E., 2009. Evidence that a secondary metabolic biosynthetic gene cluster has grown by gene relocation during evolution of the filamentous fungus *Fusarium*. Mol. Microbiol. 74, 1128–1142.

Proctor, R.H., Plattner, R.D., Desjardins, A.E., Busman, M., Butchko, R.A.E., 2006. Fumonisin production in the maize pathogen *Fusarium verticillioides*: genetic basis of naturally occurring chemical variation. J. Agric. Food Chem. 54, 2424–2430.

Rambaut, A., Drummond, A.J., 2007. Tracer v1.4. <http://beast.bio.ed.ac.uk/Tracer.

Ronquist, F., Huelsenbeck, J.P., 2003. MrBayes 3: Bayesian phylogenetic inference under mixed models. Bioinformatics 19, 1572–1574.

Rossman, A.Y., Samuels, G.J., Rogerson, C.T., Lowen, R., 1999. Genera of Bionectriaceae, Hypocreaceae and Nectriaceae (Hypocreales, Ascomycetes). Stud. Mycol. 42, 1–248.

Sanmartín, I., Enghoff, H., Ronquist, F., 2001. Patterns of animal dispersal, vicariance and diversification in the Holarctic. Biol. J. Linn. Soc. 73, 345–390.

Sarver, B.A.J., Ward, T.J., Kistler, H.C., Gale, L.R., Hilburn, K., et al., 2011. Novel *Fusarium* head blight pathogens from Nepal and Louisiana revealed by a multilocus genotyping assay and genealogical concordance. Fungal Genet. Biol. 48, 1096–1107.

Schoch, C.L., Sung, G.-H., López-Giráldez, F., Townsend, J.P., Miadlikowska, J., et al., 2009. The ascomycota tree of life: a phylum wide phylogeny clarifies the origin and evolution of fundamental reproductive and ecological traits. Syst. Biol. 58, 224–239.

Schroers, H.-J., Gräfenhan, T., Nirenberg, H.I., Seifert, K.A., 2011. A revision of *Cyanonectria* and *Geejayessia* gen. nov., and related species with *Fusarium*-like anamorphs. Stud. Mycol. 68, 115–138.

Sims, J.W., Filmore, J.P., Warner, D.D., Schmidt, E.W., 2005. Equisetin biosynthesis in *Fusarium heterosporum*. Chem. Commun. 2005, 186–188.

Skovgaard, K., Nirenberg, H.I., O'Donnell, K., Rosendahl, S., 2001. Evolution of *Fusarium oxysporum* f. sp. *vasinfectum* races inferred from multigene genealogies. Phytopathology 91, 1231–1237.

Smith, E.F., 1899. Wilt disease of cotton, watermelon, and cowpea (*Neocosmospora* nov. gen.). USDA Bull. 17, 1–54.

Smith, S.A., Beaulieu, J.M., Donoghue, M.J., 2010. An uncorrelated relaxed-clock analysis suggests an earlier origin for flowering plants. Proc. Natl. Acad. Sci. USA 107, 5897–5902.

Soltis, D.E., Bell, C.D., Kim, S., Soltis, P.S., 2008. Origin and early evolution of angiosperms. Ann. N.Y. Acad. Sci. 1133, 3–25.

Studt, L., Troncoso, C., Gong, F., Hedden, P., Toomajian, C., et al., 2012a. Segregation of secondary metabolite biosynthesis in hybrids of *Fusarium fujikuroi* and *Fusarium proliferatum*. Fungal Genet. Biol. 49, 567–577.

Studt, L., Wiemann, P., Kleigrewe, K., Humpf, H.U., Tudzynski, B., 2012b. Biosynthesis of fusarubins accounts for pigmentation of *Fusarium fujikuroi* perithecia. Appl. Environ. Microbiol. 78, 4468–4480.

Sung, G.-H., Poinar, G.O., Spatafora, J.W., 2008. The oldest fossil evidence of animal parasitism by fungi supports a cretaceous diversification of fungal-arthropod symbioses. Mol. Phylogenet. Evol. 49, 495–502.

Sutton, D.A., Brandt, M.E., 2011. *Fusarium* and other opportunistic hyaline fungi. In: Versalovic, J., Carroll, K.C., Funke, G., Jorgensen, J.H., Landry, M.L., Warnock, D.W. (Eds.), Manual of Clinical Microbiology, 10th ed. ASM Press, Washington, DC, pp. 1853–1879.

Swofford, D.L., 2003. PAUP*. Phylogenetic Analysis using Parsimony (*and other methods). Version 4. Sinauer Associates, Sunderland, Massachusetts.

Taylor, J.W., Berbee, M.L., 2006. Dating divergences in the fungal tree of life: review and new analyses. Mycologia 98, 838–849.

Taylor, J.W., Jacobson, D.J., Kroken, S., Kasuga, T., Geiser, D.M., et al., 2000. Phylogenetic species recognition and species concepts in fungi. Fungal Genet. Biol. 31, 21–32.

Thrane, U., Adler, A., Clasen, P., Galvano, F., Langseth, W., et al., 2004. Diversity in metabolite production by *Fusarium langsethiae*, *Fusarium poae*, and *Fusarium sporotrichioides*. Int. J. Food Microbiol. 95, 257–266.

Tobiasen, C., Aahman, J., Ravnholt, K., Bjerrum, M., Grell, M., et al., 2007. Nonribosomal peptide synthetase genes in *Fusarium graminearum*, *F. culmorum* and *F. pseudograminearium* and identification of NPS2 as the producer of ferricrocin. Curr. Genet. 51, 43–58.

Tudzynski, B., 2002. Biosynthesis of gibberellins in *Gibberella fujikuroi*: biomolecular aspects. Appl. Microbiol. Biotechnol. 52, 298–310.

van der Does, C., Duyvesteijn, R.G.E., Goltstein, P.M., van Schie, C.C.N., Manders, E.M.M., et al., 2008. Expression of effector gene *SIX*1 of *Fusarium oxysporum* requires living plant cells. Fungal Genet. Biol. 45, 1257–1264.

Van Hove, F., Waalwijk, C., Logrieco, A., Munaut, F., Moretti, A., 2011. *Gibberella musae* (*Fusarium musae*) sp. nov.: a new species from banana is sister to *F. verticillioides*. Mycologia 103, 570–585.

Varga, J., Kocsubé, S., Tóth, B., Mesterházy, Á., 2005. Nonribosomal peptide synthetase genes in the genome of *Fusarium graminearum*, causative agent of wheat head blight. Acta Biol. Hung. 56, 375–388.

Vasnier, C., Graziani, S., Dufresne, M., Daboussi, M.-J., 2005. Characterization of four clustered genes associated with the biosynthesis of a red perithecial pigment in *Nectria haematococca*. Fungal Genet. Newslett. 52 (Suppl.), 202.

Walker, J.D., Geissman, J.W., Compilers, 2009. Geologic time scale. Geological Society of America. http://dx.doi.org/10.1130/2009.

Ward, T.J., Bielawski, J.P., Kistler, H.C., Sullivan, E., O'Donnell, K., 2002. Ancestral polymorphism and adaptive evolution in the trichothecene mycotoxin gene, cluster of phytopathogenic *Fusarium*. Proc. Natl. Acad. Sci. USA 99, 9278–9283.

Watanabe, M., Yonezawa, T., Lee, K.-I., Kumagai, S., Sugita-Konishi, Y., 2011. Molecular phylogeny of the higher and lower taxonomy of the *Fusarium* genus and differences in the evolutionary histories of multiple genes. BMC Evol. Biol.. http://dx.doi.org/10.1186/1471-2148-11-322.

Wiemann, P., Willmann, A., Straeten, M., Kleigrewe, K., Beyer, M., et al., 2009. Biosynthesis of the red pigment bikaverin in *Fusarium fujikuroi*: genes, their function and regulation. Mol. Microbiol. 72, 931–946.

Wight, W.D., Kim, K.H., Lawrence, C.B., Walton, J.D., 2009. Biosynthesis and role in virulence of the histone deacetylase inhibitor depudecin from *Alternaria brassicicola*. Mol. Plant–Microbe Interact. 22, 1258–1267.

Wollenweber, H.W., Reinking, O.A., 1935. Die Fusarien, ihre Beschreibung, Schadwirkung, und Bekämpfung. Paul Parey, Berlin.

Wu, F., 2007. Measuring the economic impacts of *Fusarium* toxins in animal feeds. Anim. Feed Sci. Technol. 137, 363–374.

Xu, Y., Orozco, R., Wijeratne, E.M.K., Gunatilaka, A.A.L., Stock, S.P., et al., 2012. Biosynthesis of the cyclooligomer depsipeptide beauvericin, a virulence factor of the entomopathogenic fungus *Beauveria bassiana*. Chem. Biol. 15, 898–907.

Zwickl, D.J., 2006. Genetic Algorithm Approaches for the Phylogenetic Analysis of Large Biological Sequence Datasets Under the Maximum Likelihood Criterion. Ph.D. Dissertation. The University of Texas at Austin.